

# Physics at high $Q^2$ at HERA

Trong Hieu TRAN  
DESY, Hamburg

On behalf of the  
H1 and ZEUS collaborations

Photon 2011, Spa, Belgium

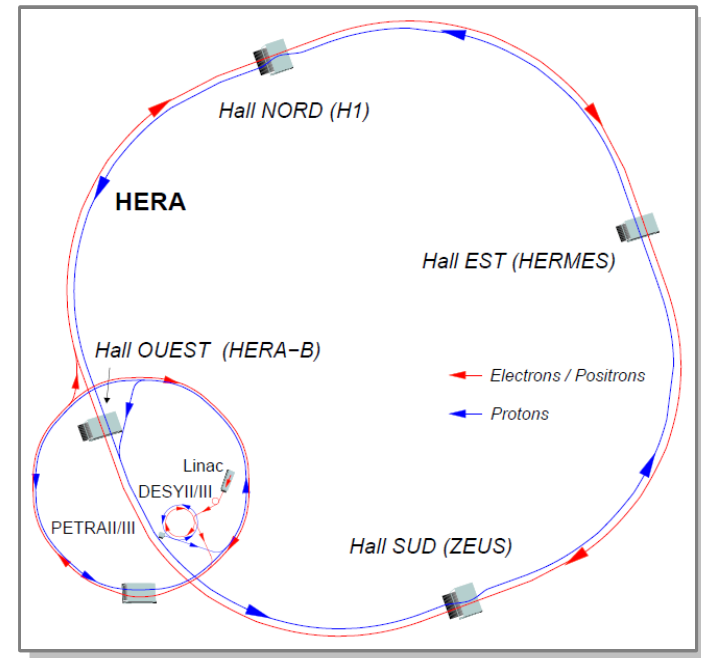
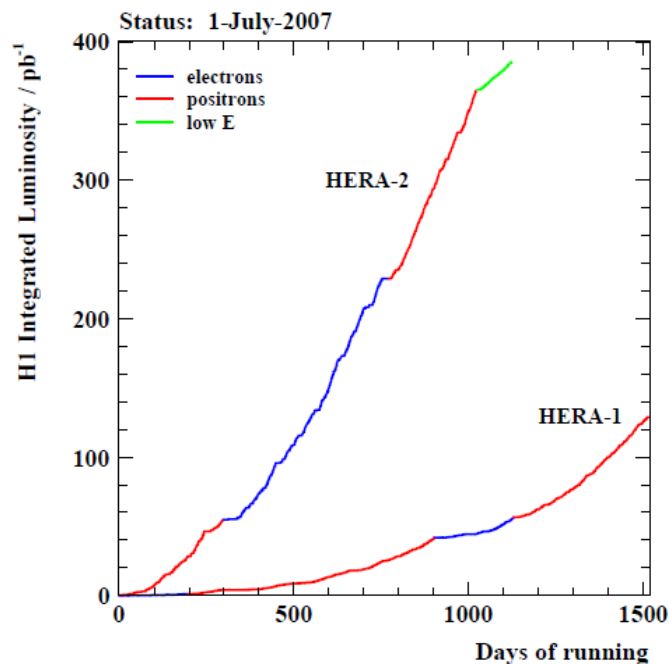
## Outline:

- H1 and ZEUS at HERA
- Deep inelastic scattering
- Recent results on high  $Q^2$  physics at HERA



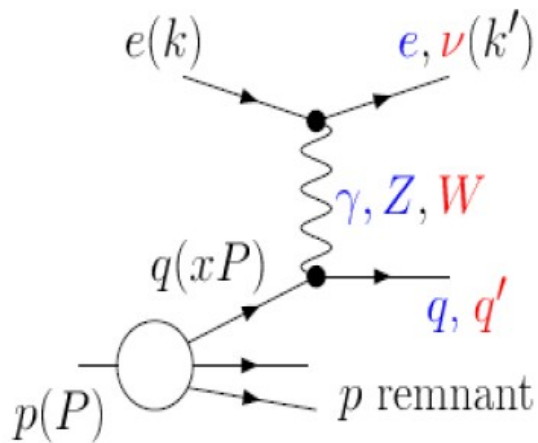
# HERA

- The world most powerful electron microscope, located in Hamburg, Germany
- Two collider experiments at the ep interaction points
- Center-of-mass energy: 225-319 GeV
- HERA-II: longitudinal polarised electrons (positrons)



- Integrated luminosity of 0.5 fb<sup>-1</sup> per experiment
- Studies of Electroweak physics, BSM, ...

# Deep Inelastic Scattering (DIS)



## DIS kinematics

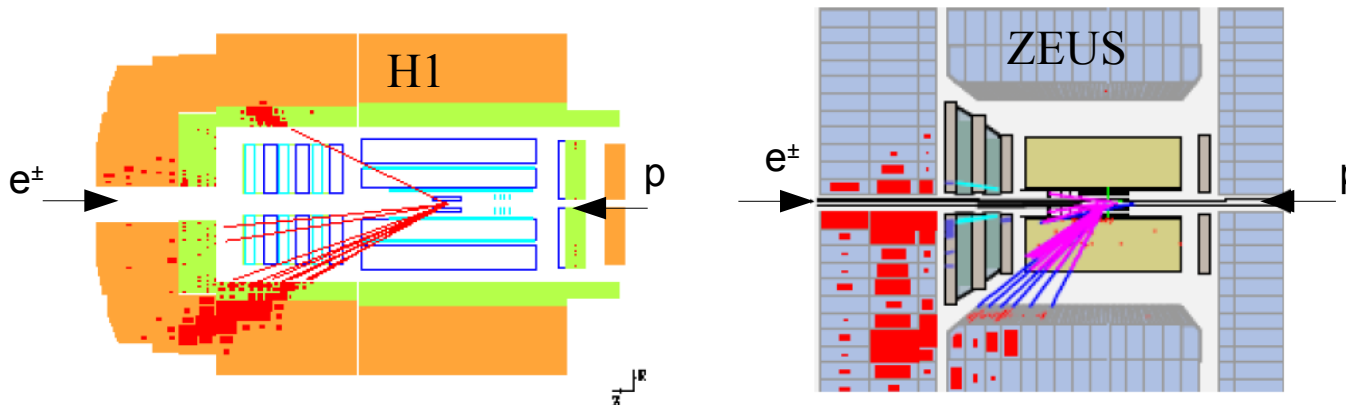
$$Q^2 = -q^2 = (k - k')^2, \quad Q^2 \in [0, s]$$

$$x = \frac{Q^2}{2P \cdot q}, \quad x \in [0, 1]$$

$$y = \frac{q \cdot P}{k \cdot P}, \quad y \in [0, 1]$$

- $Q^2$ : virtuality of the exchanged boson
- $x$ : momentum fraction carried by struck quark
- $y$ : inelasticity

HERA covers a wide kinematic range, up to five orders in magnitude in log-scale of  $Q^2$ .



Example of neutral current (H1) and charged current (ZEUS) events.

# Deep Inelastic Scattering: cross section

- DIS neutral current (NC) cross section is expressed using proton structure functions

$$\frac{d^2\sigma_{\text{NC}}^{\pm}}{dx dQ^2} = \frac{4\pi\alpha_s^2}{Q^4} \left[ Y_+ \tilde{F}_2 - y^2 \tilde{F}_L \mp Y_- x \tilde{F}_3 \right]$$

$Y_{\pm} = 1 \pm (1 - y)^2$   
helicity function

dominant contribution      sizable at high  $Y$       important at high  $Q^2$

➡ Polarisation dependence due to  $\gamma Z$  interference term

$$\begin{aligned} \tilde{F}_2 &= F_2 - (v_e - P_e a_e) \kappa_Z F_2^{\gamma Z} + (v_e^2 + a_e^2 - 2P_e v_e a_e) \kappa_Z^2 + F_2^Z \\ x \tilde{F}_3 &= -(a_e - P_e v_e) \kappa_Z x F_3^{\gamma Z} + [2v_e a_e - P_e (v_e^2 + a_e^2) \kappa_Z^2 x F_3^Z] \end{aligned}$$

$$P_e = \frac{N_R - N_L}{N_R + N_L}$$

- Charged current (CC) cross section

$$\frac{d^2\sigma_{\text{CC}}^{\pm}}{dx dQ^2} = \frac{G_F^2}{4\pi x} \left[ \frac{M_W^2}{Q^2 + M_W^2} \right]^2 \left[ Y_+ F_2^{\pm \text{CC}} - y^2 F_L^{\pm \text{CC}} \mp Y_- x F_3^{\pm \text{CC}} \right]$$

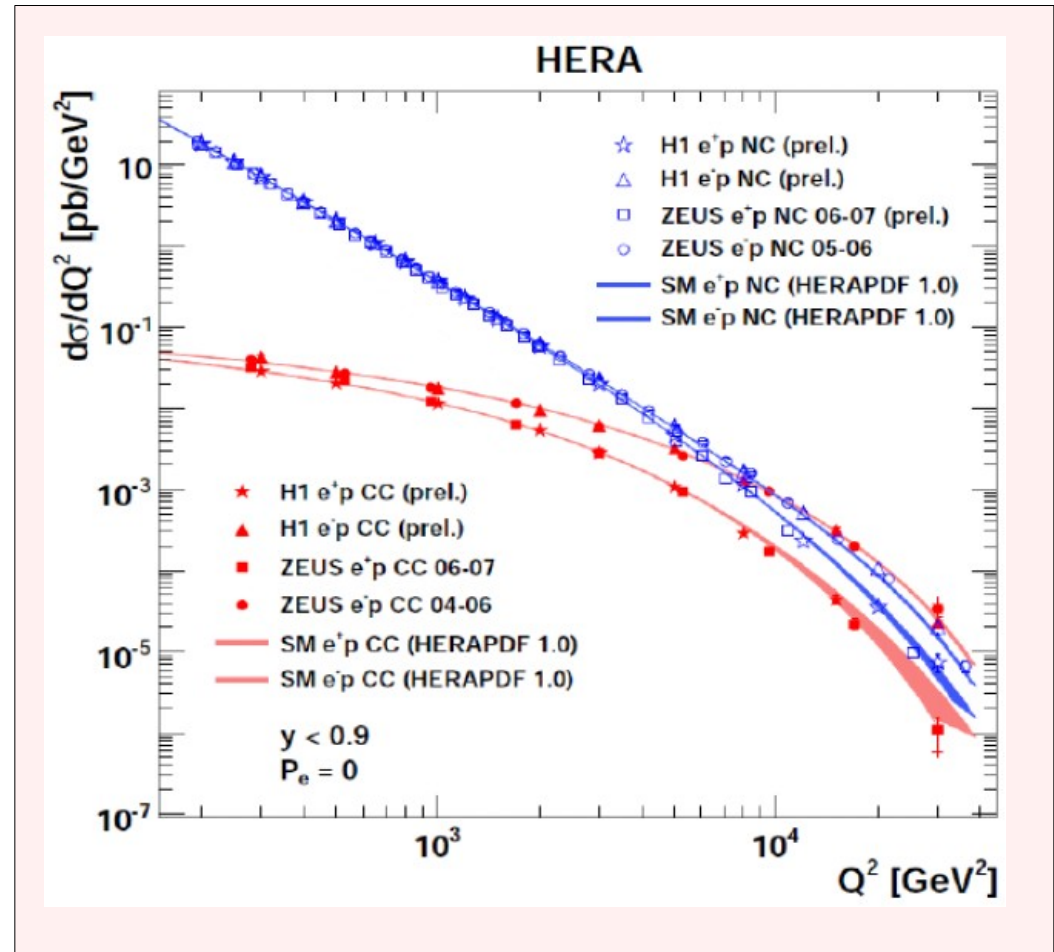
CC cross section for  $e^-$ ,  $e^+$  sensitive to different type of quark

# HERA I+II unpolarized DIS cross section

At low  $Q^2$ :  $\sigma_{\text{NC}}(e^+p) \approx \sigma_{\text{NC}}(ep)$   
due to photon exchange.  
Charged current events are  
suppressed by massive  $W$ -  
boson

At high  $Q^2$ ,  
 $\sigma_{\text{CC}}(ep) > \sigma_{\text{CC}}(e^+p)$ , due to  $W^-$  ( $W^+$ )  
exchange which couple to up  
(down) type quark.

Diffence of NC cross section for  
electron and positron due to  
interference  $\gamma$  -  $Z$  boson.



HERA data allow a visualization of the "unification" of the electromagnetic and weak interactions at  $W$ - $Z$  scale.

# $x\tilde{F}_3^{\gamma Z}$ – interference of $\gamma$ and Z-boson

The expression for  $x\tilde{F}_3(x, Q^2)$  is related to the reduced NC cross sections

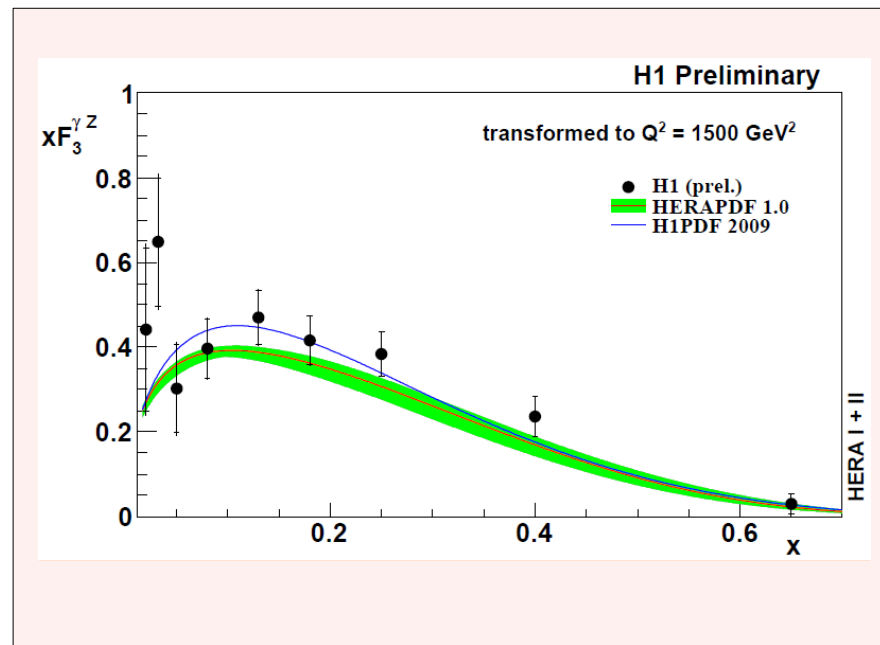
$$x\tilde{F}_3^{\pm}(x, Q^2) = -a_l P_Z x\tilde{F}_3^{\gamma Z}(x) + 2a_l v_l P_Z^2 x\tilde{F}_3^Z(x)$$

$$P_Z = \frac{Q^2}{Q^2 + M_Z^2} \frac{1}{\sin(2\theta_W)}$$

dominant contribution to  $x\tilde{F}_3(x, Q^2)$  arises  
from the  $\gamma$  - Z interference term:  $x\tilde{F}_3^{\gamma Z}$

a, v: axial & vector  
coupling of the lepton

$x\tilde{F}_3^{\gamma Z}$  : little dependence on  $Q^2 \rightarrow$  transformation to one  $Q^2$  value.



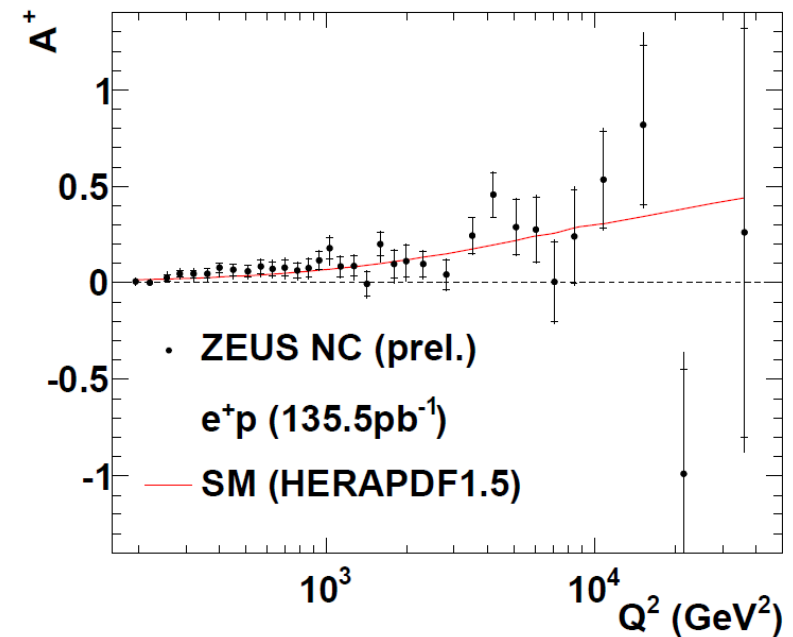
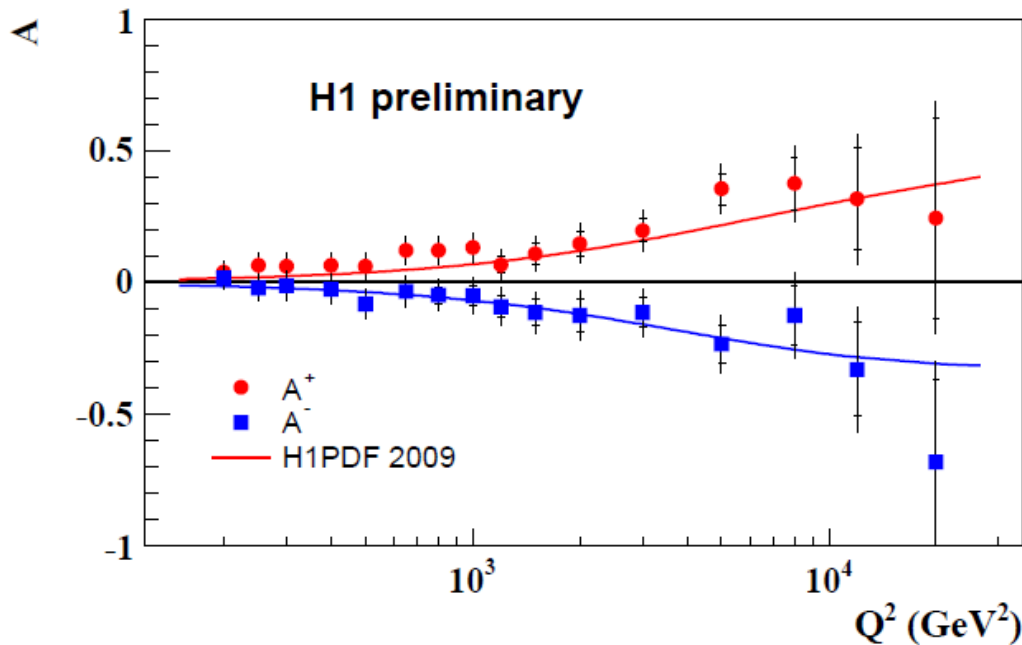
# Neutral current polarisation asymmetry

Polarization asymmetry

$$A = \frac{2}{P_R - P_L} \cdot \frac{\sigma^\pm(P_R) - \sigma^\pm(P_L)}{\sigma^\pm(P_R) + \sigma^\pm(P_L)}.$$

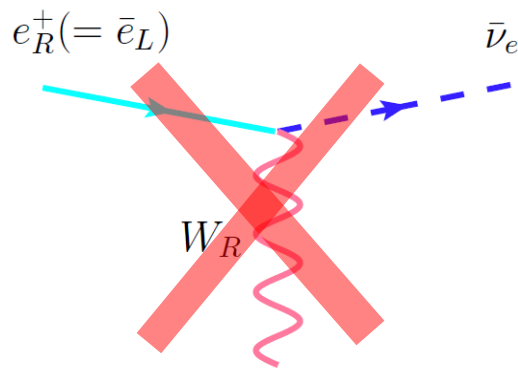
$$b^e = \frac{v_L^e + v_L^e}{v_L^e - v_L^e}$$

At high  $Q^2$ , the difference between  $A$  values for  $e^+p$  and  $e^-p$  interaction becomes important due to the  $Z$ -boson exchange.

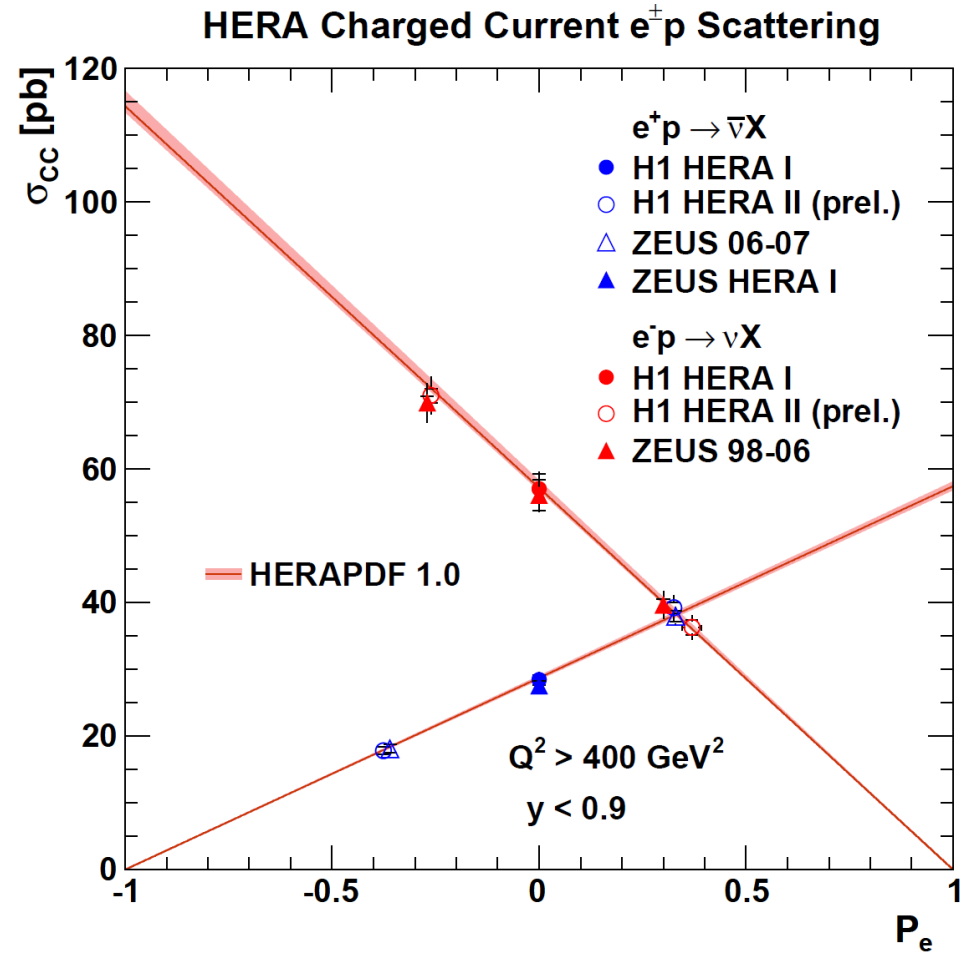


# Charged current total cross section

- ◆ Charged current interaction affect only left-handed particles
- ◆ Cross section varies linearly in function of polarisation



- ◆ Good agreement with SM prediction.
- ◆ Difference at  $P_e = -1$  will be used to constraint  $M_{W_R}$ .  
( $M_{W_R} > 198 \text{ GeV}$  from final ZEUS result. )

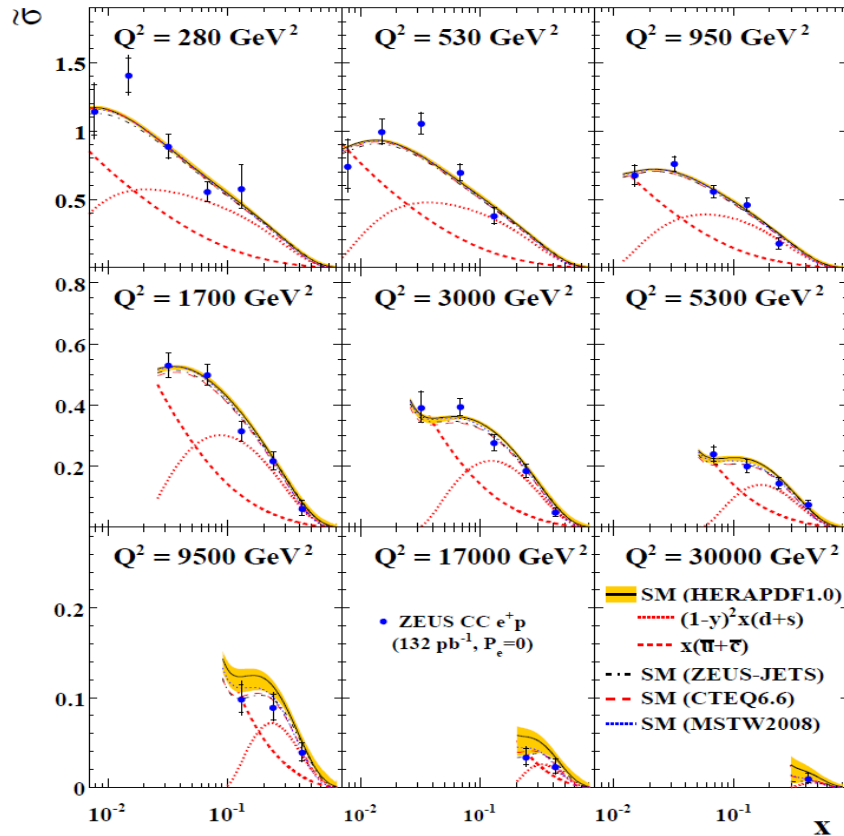




# Charged current reduced cross section

positron

ZEUS

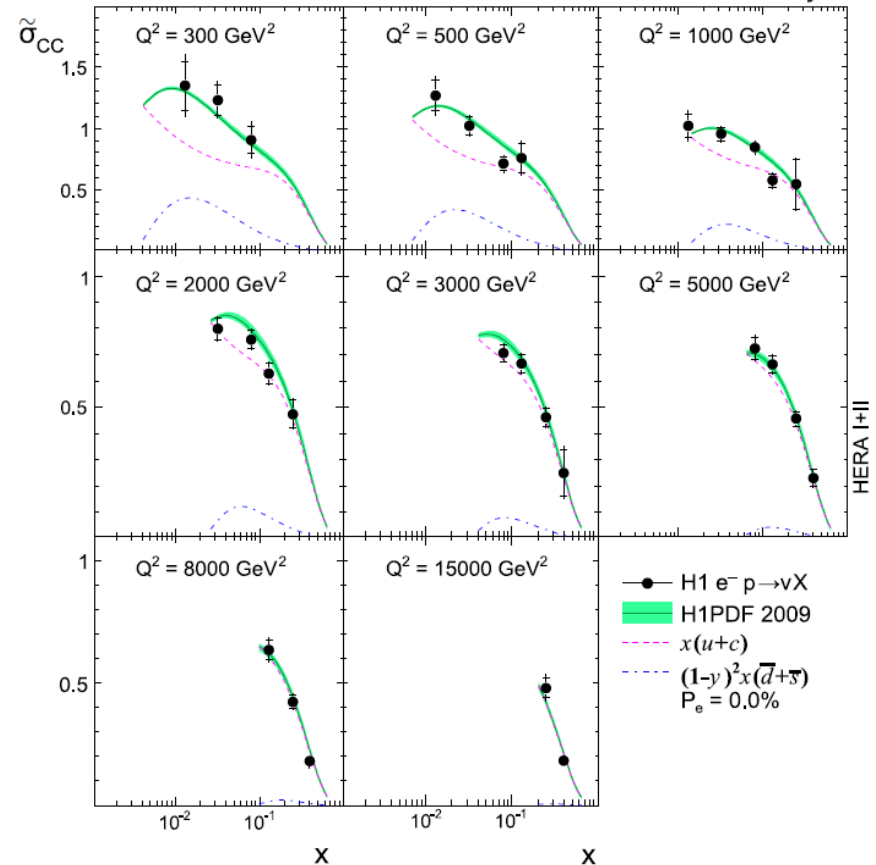


$$\tilde{\sigma}_{CC}^+ \approx x[\bar{u} + \bar{c} + (1-y)^2(d+s+b)]$$

➤ PDF of d-quark dominates  $e^+p$  cross section at high  $x$

electron

H1 Preliminary

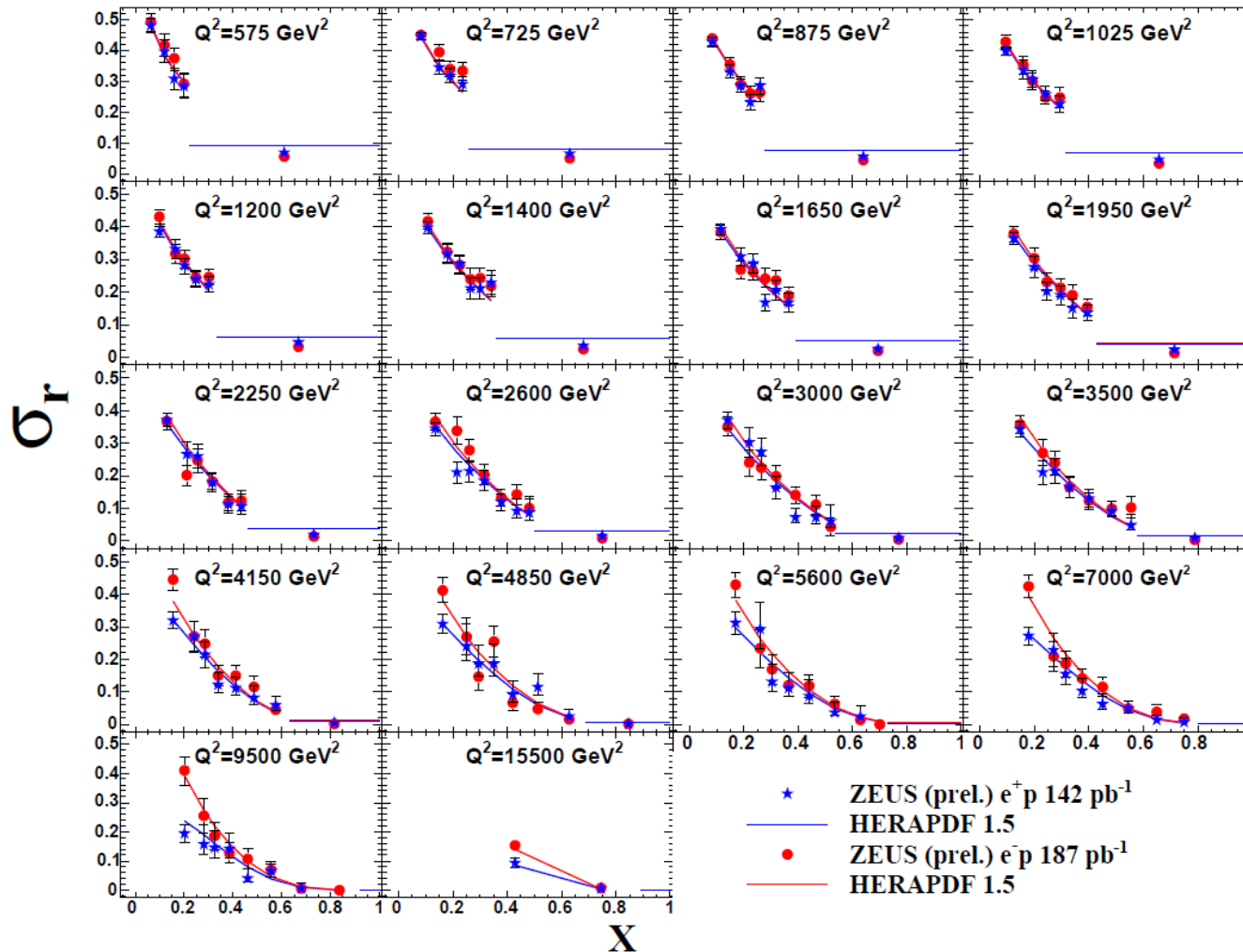


$$\tilde{\sigma}_{CC}^- \approx x[u + c + (1-y)^2(\bar{d} + \bar{s} + \bar{b})]$$

➤ PDF of u-quark dominates  $e^-p$  cross section

# Neutral current reduced cross section

ZEUS



NC measurement at high  $x$   
(up to 1)

$x$  reconstruction relies on  
jets force jets to balance  
 $p_T$  of electron yields better  
 $x$  resolution.

New method allows access  
to the very high  $x$  region  
not accessible so far at  
HERA.

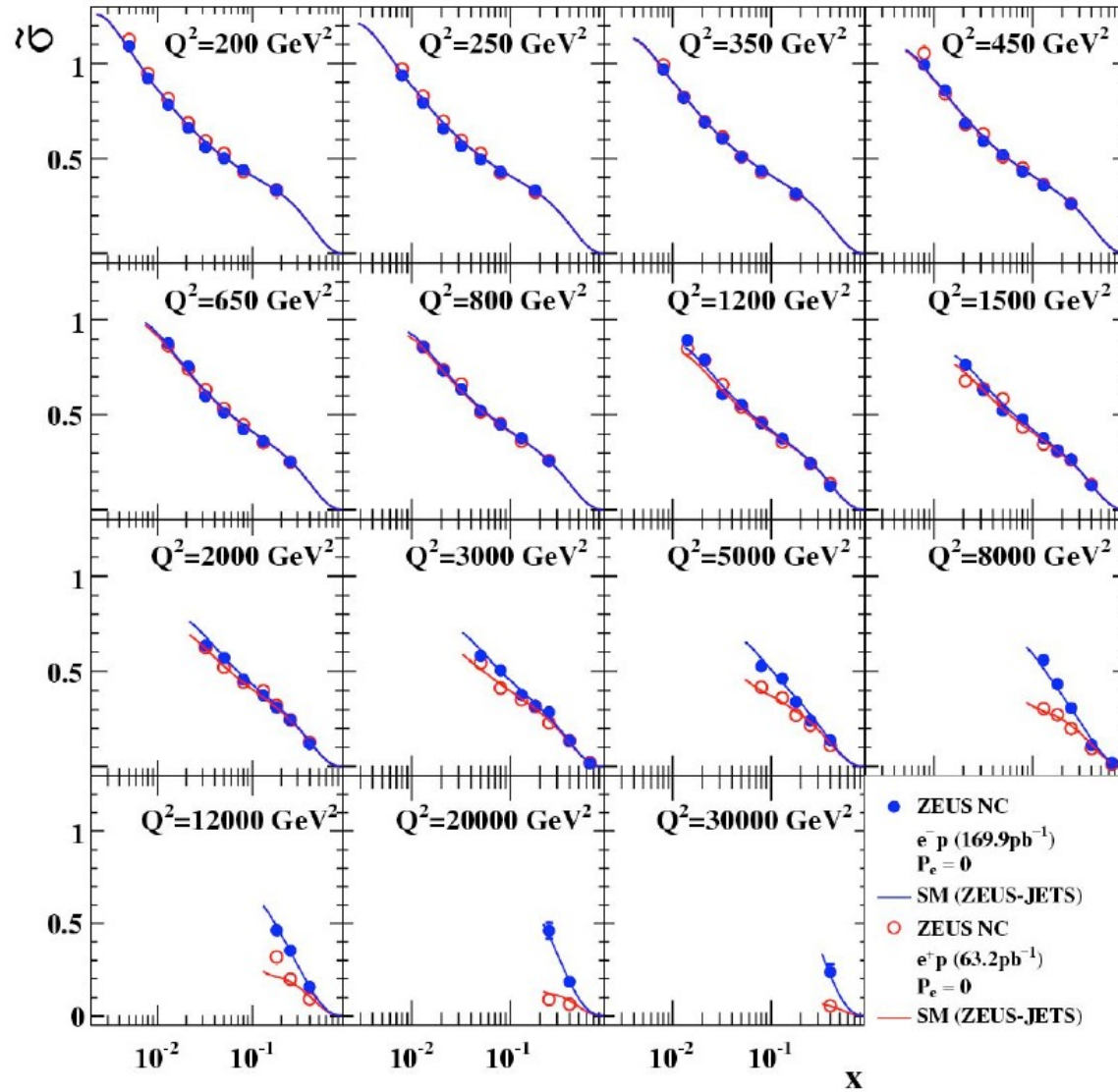
# Summary

- Success of HERA operation are shown in many precision measurements.
- Recent results from study of deep inelastic scattering
  - ◆ Electroweak unification is confirmed by neutral and charged current cross section at high  $Q^2$ .
  - ◆ Polarisation asymmetry in both NC and CC interaction.
  - ◆ Interference of  $\gamma$  to Z-boson was measured via structure function  $x F_3^{\gamma Z}$ .
  - ◆ CC data are compatible with the absent right handed currents
- Many results from HERA are still coming in the next few years including H1-ZEUS combinations.

# Extra slides

# Unpolarised reduced NC cross section

## ZEUS



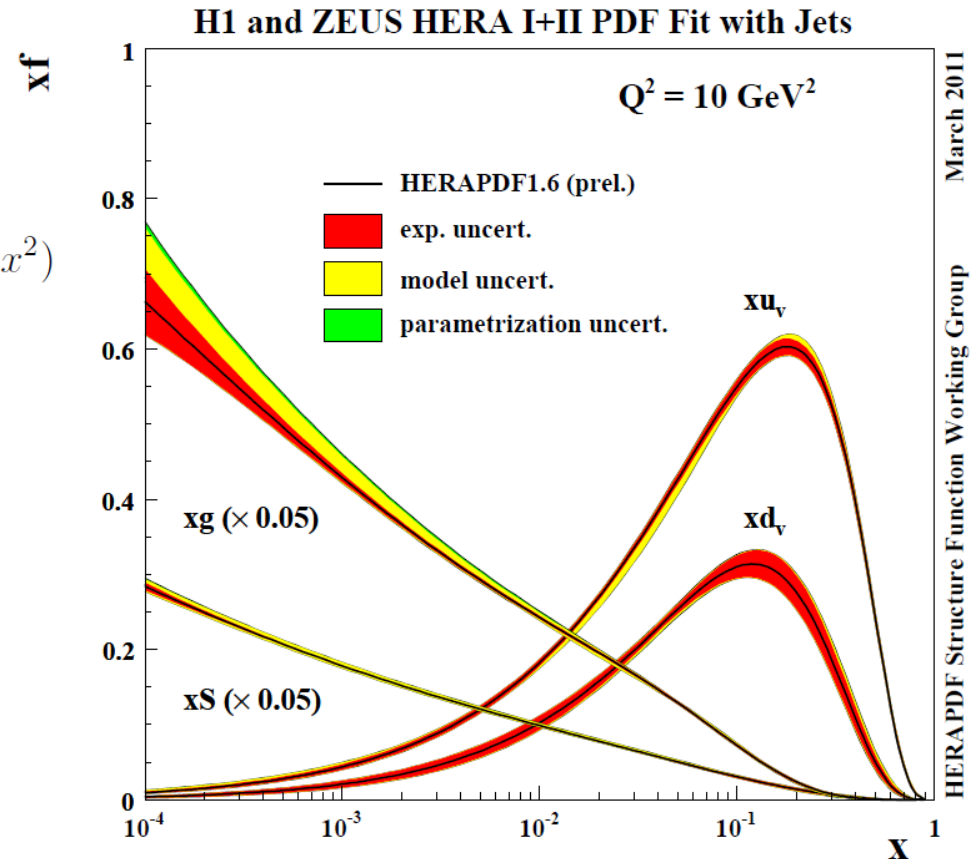
Separation of  $e^+p$  and  $e^-p$  cross sections at high  $Q^2$  due to  $\gamma Z$  interference term.

Visible difference in the  $e^+p$  and  $e^-p$  cross sections is well described by the SM predictions

# HERAPDF 1.6 with jets

## HERAPDF 1.6 parametrisation

$$\begin{aligned}
 xg(x) &= A_g x^{B_g} \cdot (1-x)^{C_g} - A'_g x^{B'_g} (1-x)^{C'_g} \\
 xu_v(x) &= A_{u_v} x^{B_{u_v}} \cdot (1-x)^{C_{u_v}} \cdot (1 + D_{u_v} x + E_{u_v} x^2) \\
 xd_v(x) &= A_{d_v} x^{B_{d_v}} \cdot (1-x)^{C_{d_v}} \\
 x\bar{U}(x) &= A_{\bar{U}} x^{B_{\bar{U}}} \cdot (1-x)^{C_{\bar{U}}} \\
 x\bar{D}(x) &= A_{\bar{D}} x^{B_{\bar{D}}} \cdot (1-x)^{C_{\bar{D}}}
 \end{aligned}$$



Parton density functions for HERAPDF1.6 as a function of  $x$  for  $Q^2 = 10 \text{ GeV}^2$ . The central value (solid line) is shown together with the experimental, model and parametrization uncertainties represented by the red, yellow and green shaded bands, respectively.